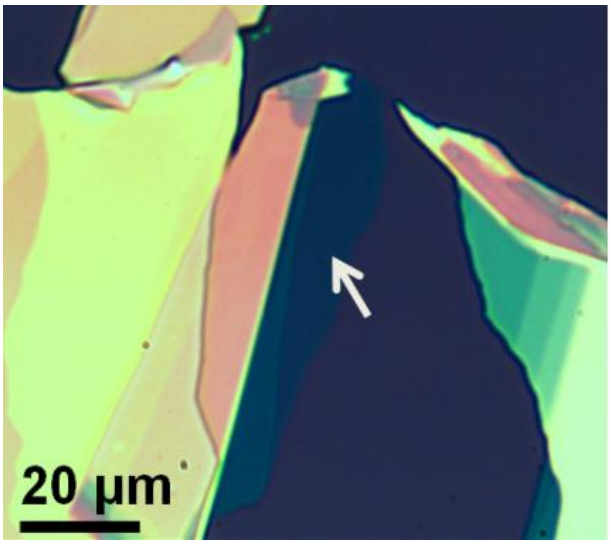

Supplementary Figure S1. Optical image of a few layers MoS_2 flake on the SiO_2 substrate. Its thinnest region is labeled by white arrow.

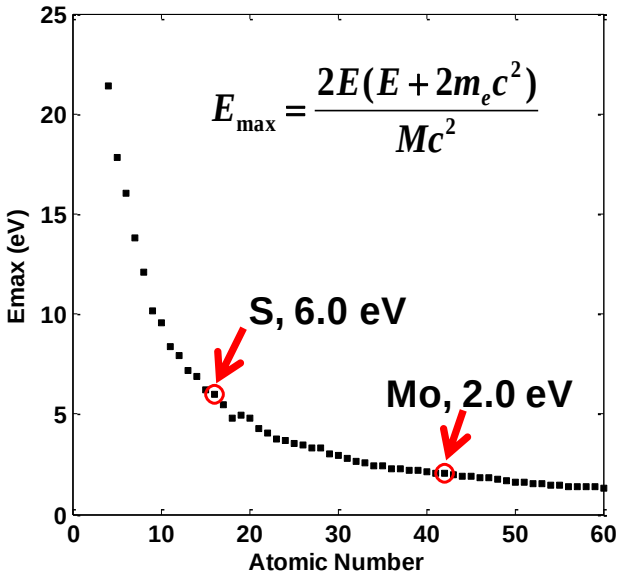

Supplementary Figure S2. Maximum energy transferred from an 80 keV incident electron to various atoms. Although the maximum transferred energy to S atom (6.0 eV) is less than the threshold for displacing S atom from pristine MoS_2 sheet (6.9 eV), S atom could also be knocked out from the lattice when lattice vibration and ionization are accounted for, which provides the basis for forming of initial vacancies and pores. The displacement energy for unsaturated S atoms is less than 6.0 eV, which means that S atoms are sputtered fairly easily from the edges of nanostructures. Although Mo atoms are hardly displaced by electrons, Mo atoms would release and aggregate at the edge when all adjacent S atoms are knocked out.

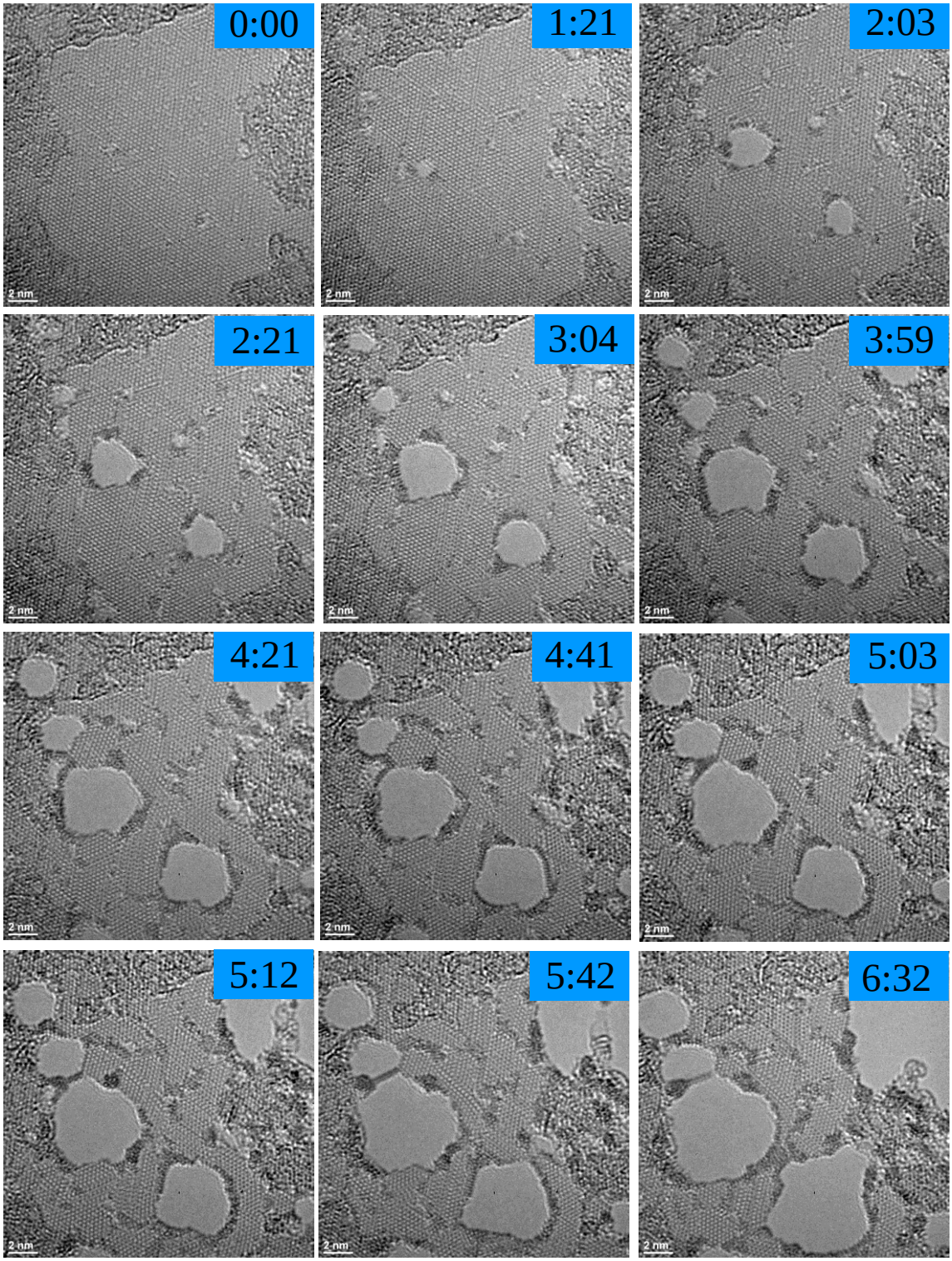

Supplementary Figure S3. Time series of HRTEM images of a MoS_2 monolayer under electron irradiation. Nanopores formed and grew from initial defects under electron irradiation. Eventually, a narrow ribbon formed between two adjacent pores (at 5:03) and kept elongating for minutes.

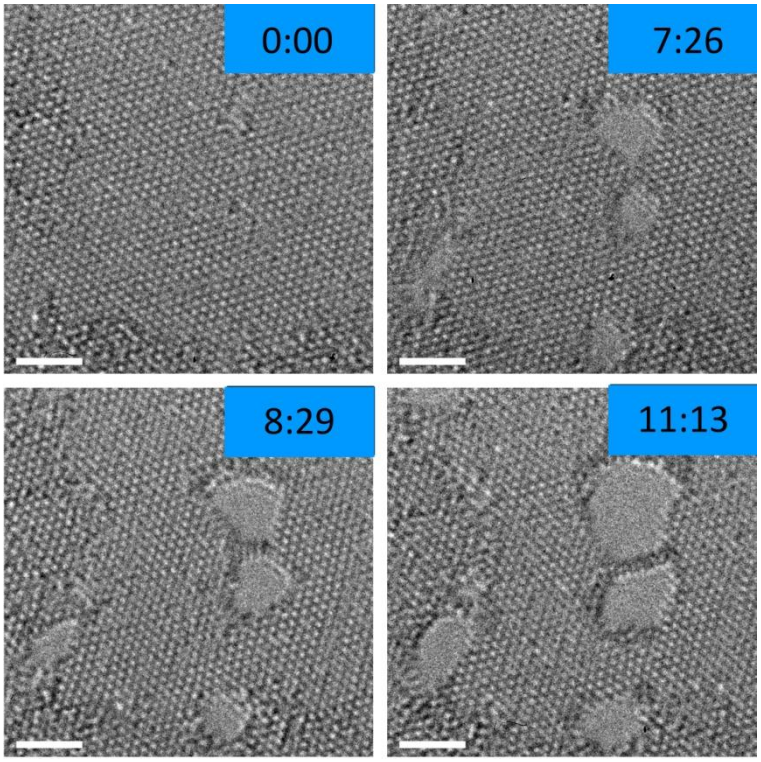

Supplementary Figure S4. Another narrowest ribbon derived from monolayer MoS_2. The scale bar is 2 nm.

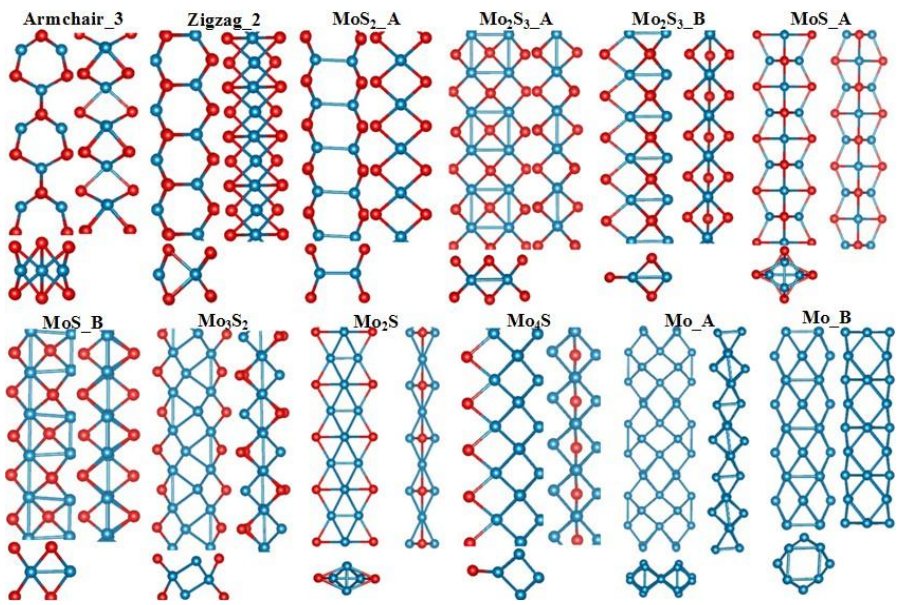

Supplementary Figure S5. **Three view depictions of the optimized ribbon candidates for the fine molybdenum sulfide ribbon other than Mo_5S_4, as summarized in Supplementary Table S1**. The cyan and red atoms stand for molybdenum and sulfur. According to the experimental HRTEM graph of the fine ribbon (Fig. 2a), we mainly consider ribbon structures with at most three columns of atoms in each cross section. As the ribbon is a Mo-rich structure (Fig. S5), ribbons with ratio of molybdenum to sulfur ranging from 2:1 to 1:0 are theoretically investigated here.

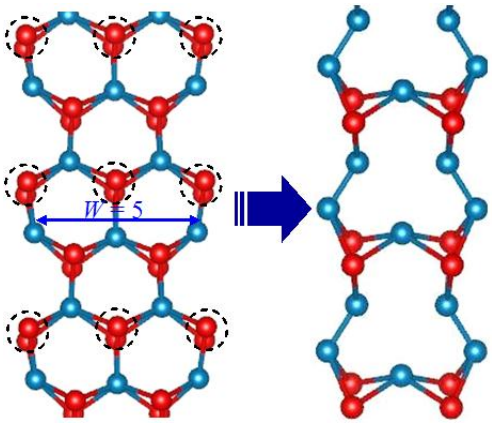

Supplementary Figure S6. Selection of the initial structure for the simulation of phase transition into Mo_5S_4 ribbon. The right structure is the S-impoverished ribbon used as the initial structure for the simulation of phase transition, which is presumed by removing six S atoms per unit cell from the MoS_2 armchair ribbon of five dimer lines. The width *W* stands for the number of the dimer lines in width direction. The removed S atoms are labeled by black dashed circles.

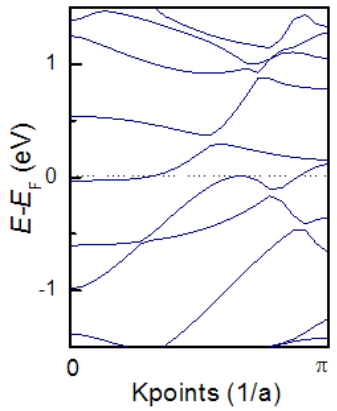

Supplementary Figure S7. Electronic band structure of the Mo_5S_4 nanoribbon calculated without considering the axial reconstruction of two unit cells. This band structure reflects that the fine ribbon is a metal without Peierls distortion of the 1D structure.

Supplementary Table S1. Cohesive energies and lattice constants of possible narrowest Mo-S ribbons.

Ribbon structure		Cohesive energy (eV/atom)	Axial constant (Å)	Distance between two Mo columns (Å)
MoS_2	Armchair_3	-4.20	5.25	-
	Zigzag_2	-4.36	3.09	1.87
	A	-4.36	2.99	2.51
Mo_2S_3	A	-4.82	2.77	2.69
	B	-4.41	2.98	2.62
MoS	A	-4.90	4.50	2.55
	B	-4.45	5.22	2.52
Mo_5S_4		-4.91	4.54	2.80
Mo_3S_2		-4.78	2.89	2.87
Mo_2S		-4.62	4.40	2.28
Mo_4S		-4.48	3.05	2.83
Mo	A	-4.49	3.35	3.12
	B	-4.22	3.80	2.56/2.87

The cohesive energy of ribbon with respect to the chemical potential of single Mo and S atoms is defined as $(E_{ribbon} - n_{Mo} \times \mu_{Mo} - n_S \times \mu_S)/n_{total}$, where E_{ribbon}, μ_{Mo}, μ_S are energies of ribbon, isolated Mo and isolated S, and n_{Mo}, n_S and n_{total} are the numbers of Mo, S and total atoms. The cohesive energy for MoS_2 monolayer is calculated to be -5.17 eV/atom. The axial constant and distance between two inner columns of atom estimated from TEM are 4.6 and 2.7 Å respectively. The atomic structures of the ribbons are depicted in Supplementary Figure S6.